

T_g, density and X-ray diffraction of zinc-doped bioactive glasses with molar formulation : 20.15[(2.038+x)SiO₂-(1.457-x)Na₂O]-2.6P₂O₅-26.905CaO-0.045ZnO system

ABSTRACT

In the present work, glasses with molar composition 20.15[(2.038+x)SiO₂-(1.457-x)Na₂O]-2.6P₂O₅-26.905CaO-0.045ZnO were studied in order to contribute to the application of thermal analysis methods to the characterization of zinc-doped bioactive glasses. The aim is to provide answers to the expectations of practitioners before *in vitro* or *in vivo* tests on the physicochemical properties of these zinc doped bioactive glasses. Samples were produced by high temperature melting followed by quenching. The samples were characterized by X-ray diffraction (XRD), differential scanning calorimetry (DSC) and pycnometry. The results show that the samples are amorphous, and the values for vitreous transition temperature and density are of the same order of magnitude as those for the system without addition of ZnO. Consequently, it appears that the addition of 0.045 % mol of ZnO to the base glass does not significantly alter the physicochemical and structural properties of the glass.

Keywords: Bioactive glass, Structure, Glass transition temperature, Density, DSC

1. INTRODUCTION

The increase in life expectancy is accompanied by a deterioration in general health and an increase in chronic diseases as people age. Among these manifestations of ageing, damage to the musculoskeletal system is particularly disabling and considerably accelerates the onset of dependence. Worldwide, 2.2 million bone grafts are performed each year, but the rate of post-operative complications remains high and is estimated at 15 % of interventions (Menci et al., 2019).

When a bone deficit exceeds a critical size as a result of fractures or degeneration, autologous, allogeneous or xenogeneous grafts become almost ineffective when rapid repair of the deficit site is necessary and consequently spontaneous and rapid regeneration is required. of the organism (Menci et al., 2019). Synthetic materials known as biomaterials, available in various dimensions and in large quantities, offering an attractive alternative to this lack, are currently being developed.

These biomaterials, and specifically SiO₂-P₂O₅-Na₂O-CaO bioactive glasses, are attracting growing biomedical interest because they undeniable qualities for the development of such functions : easy shaping, low cost and above all, a great diversity of composition and resistance to ageing. They have the property of forming an apatite layer both on the surface of a physiological liquid (*in vitro*) and in a living environment (*in vivo*) (Jebahi et al., 2012). This particularity of being both bioactive and biocompatible opens up a wide range of applications, in particular, the filling of bone defects in orthopedic surgery (head of hip or knee prosthesis) or dental surgery (dental prosthesis).

Since their appearance, other glass and ceramic glass compositions have been developed to enhance the properties and clinical capabilities of traditional bioactive glass. One trend is the incorporation of trace elements into the composition of these bioactive glasses and ceramic glasses (magnesium, strontium, zinc...) to improve their physical characteristics and ensure therapeutic benefit (Andersson et al, 1998).

In this perspective, zinc-doped bioactive glasses have been used. Zinc plays an important role in bone cell multiplication as well as the production of collagen in the bone structure (Dickey *et al.*, 2013). Zinc could also contribute to improving bone mineral density in cases of osteoporosis (Tokudome & Otsuka 2012). Porosity allows good tissue invasion (Diaye *et al.*, 2013). Thus, the addition of ZnO to bioactive glasses stimulates cell proliferation and differentiation and facilitates the development of a durable bond with bone (Feng *et al.*, 2014). Then, the presence of zinc oxide in bioactive glass, improves its mechanical strength (Chajri *et al.*, 2016, Ouis, 2011) and chemical durability or reduces its degradability in aqueous solutions such as SBF.

The present work is part the context of a study of the physicochemical properties of zinc doped bioactive glasses with a view to providing answers to the expectations of practitioners before in vitro or in vivo tests. The aim of this contribution is to apply thermal analysis methods to the characterization of zinc-doped bioactive glasses.

2. MATERIAL AND METHODS

The glasses of formulation $20.15[(2.038+x)\text{SiO}_2-(1.457-x)\text{Na}_2\text{O}]-2.6\text{P}_2\text{O}_5-26.905\text{CaO}-0.045\text{ZnO}$, $0 \leq x \leq 1$ in steps of 0.125 were synthesized from commercial products whose characteristics of origin and purity are shown in **Table 1**.

Table 1. Name, formula, origin and purity of products used

Réactifs	Formule	Provenance	Pureté (%)
Sodium silicate	Na_2SiO_3	Alfa Aesar	99,0
Calcium pyrophosphate	$\text{Ca}_2\text{P}_2\text{O}_7$	Aldrich	99,9
Calcium phosphate	$\text{Ca}_3(\text{PO}_4)_2$	Prolabo	99,5
Silica	SiO_2 quartz α	Merck	99,9
Zinc oxide	ZnO	Merck	99,0
Diethyl ortho-phthalate	$\text{C}_{12}\text{H}_{14}\text{O}_4$	Merck	99,0

Reagent powders were weighed using a Sartorius brand balance with a precision of 0.01 mg. They were then mixed and finely ground ($<50 \mu\text{m}$) in the chosen proportions in an agate mortar in the presence of ethanol in order to obtain a homogeneous distribution in the mixture and maximum contact between the grains, thus facilitating vitrification. The resulting mixture is placed in a platinum crucible. It is brought into an oven to undergo a thermal cycle following the temperature programming defined on the profile described in **Figure 1**.

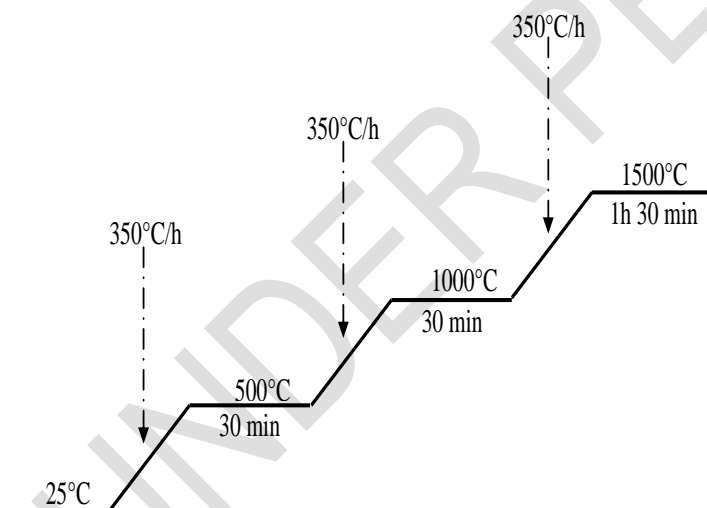


Fig. 1. Heat treatment cycle of the reagents used

After complete melting, the sample is obtained by dipping the bottom of the crucible in water at room temperature. This almost instantaneous cooling produces glass fragments. These glass fragments are then stored in a dry atmosphere in a

desiccator in the presence of P_2O_5 . Nominal compositions expressed in molar and mass percentages are shown in **Table 2**.

Table 2. Compositions in molar and mass percentages (in brackets) of processed samples

x	SiO ₂	P ₂ O ₅	Na ₂ O	CaO	ZnO
0	41,08 (40,00)	2,60 (5,98)	29,37 (29,50)	26,905 (24,46)	0,045 (0,06)
0,125	43,60 (42,48)	2,60 (5,99)	26,85 (26,99)	26,905 (24,48)	0,045 (0,06)
0,25	46,12 (44,97)	2,60 (5,99)	24,33 (24,48)	26,905 (24,50)	0,045 (0,06)
0,375	48,63 (47,46)	2,60 (6,00)	21,81 (21,96)	26,905 (24,52)	0,045 (0,06)
0,5	51,15 (49,96)	2,60 (6,00)	19,29 (19,44)	26,905 (24,54)	0,045 (0,06)
0,625	53,67 (52,47)	2,60 (6,01)	16,77 (16,91)	26,905 (24,55)	0,045 (0,06)
0,75	56,19 (54,98)	2,60 (6,01)	14,25 (14,38)	26,905 (24,57)	0,045 (0,06)
0,875	58,71 (57,48)	2,60 (6,02)	11,73 (11,85)	26,905 (24,59)	0,045 (0,06)
1	61,23 (60,00)	2,60 (6,02)	9,21 (9,31)	26,905 (24,61)	0,045 (0,06)

In order to characterize the structural state (crystalline or amorphous), powder measurements of the samples were carried out by X-ray diffraction using a D5000 SIEMENS Brücker type diffractometer ($Cu_{K\alpha}$ line), goniometer θ , equipped with a copper anticathode tube with a wavelength $\lambda = 1.5406 \text{ \AA}$. The spectrum was taken in the 2θ range from 10° to 60° with a step size of 0.02° and a scan speed of $2^\circ / \text{min}$. Experiments were carried out at 25°C . A $50 \text{ }\mu\text{m}$ particle size powder was used.

The glass transition temperature (T_g) was determined using a DSC 111-SETARAM calorimeter. The device is fitted with a crimped stainless steel crucible containing the sample to be analyzed and a reference, which may contain thermally inert material or remain empty. Glass powders with a mass of 30 mg and a size of approximately $100 \text{ }\mu\text{m}$ were placed in crimped stainless steel crucibles. Experiments were carried out under an argon atmosphere and at a heating rate of $5^\circ\text{C}/\text{min}$ from 25 to 700°C . This technique was used by Kouyate *et al* (2013). Glass transition temperature (T_g) was determined with an accuracy of $\pm 3^\circ\text{C}$ for each sample.

Glass sample densities were estimated at 296.15 K using a pycnometer with diethyl phthalate ($d = 1.118$) as the immersion liquid with an accuracy of $\pm 0.03 \text{ g.cm}^{-3}$.

3. RESULTS AND DISCUSSION

3.1 Results

Figure 2 shows some X-ray diffractograms of the $20.15[(2.038+x)\text{SiO}_2-(1.457-x)\text{Na}_2\text{O}]-2.6\text{P}_2\text{O}_5-26.905\text{CaO}-0.045\text{ZnO}$ glass formulations. No acute peak of diffraction was not observed on any of the diffractograms, but a diffraction halo around $2\theta = 33^\circ$.

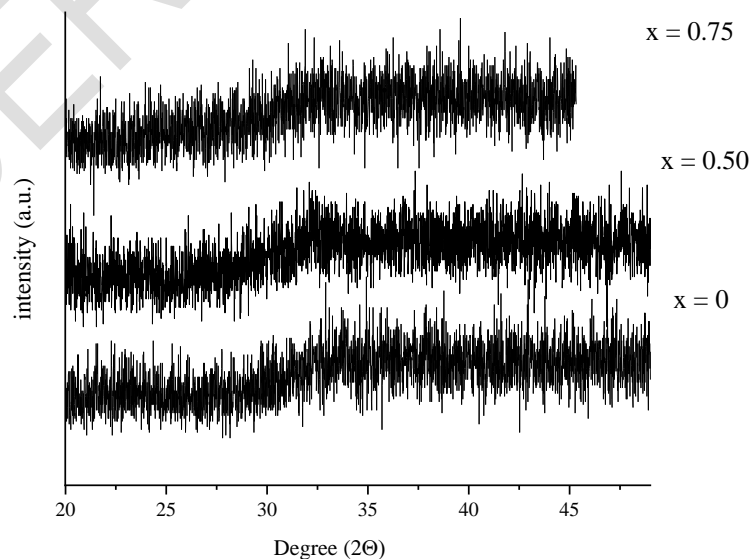


Fig.2.X-ray diffractograms of some glass compositions with molar formula $20.15[(2.038+x)\text{SiO}_2-(1.457-x)\text{Na}_2\text{O}]-2.6\text{P}_2\text{O}_5-26.905\text{CaO}-0.045\text{ZnO}$; $0 \leq x \leq 1$

The thermograms are shown in Figure 3. Each of these thermograms exhibits a unique glass transition. These data show endothermic effects in the temperature range of 484-607°C.

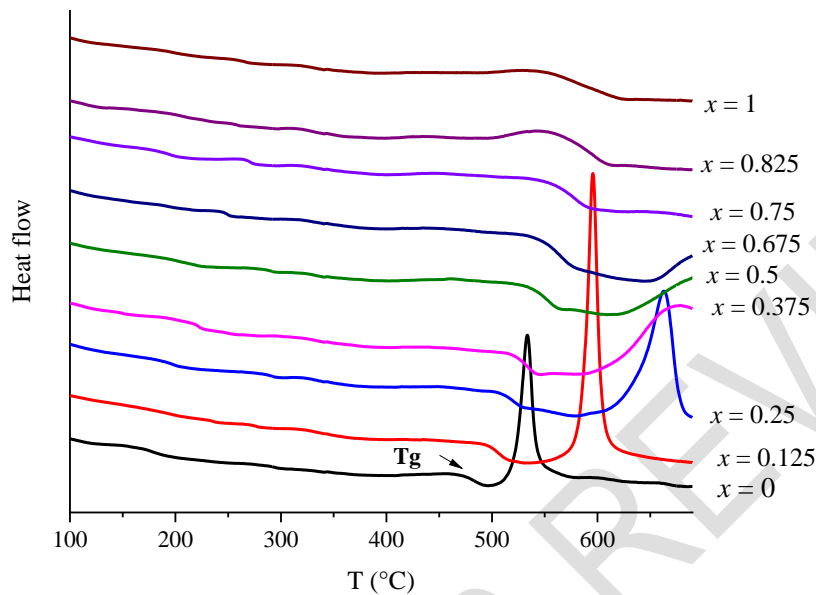


Fig.3.Thermograms of glasses from the $20.15[(2.038+x)\text{SiO}_2-(1.457-x)\text{Na}_2\text{O}]-2.6\text{P}_2\text{O}_5-26.905\text{CaO}-0.045\text{ZnO}$ system; $0 \leq x \leq 1$

Measurements of the glass transition temperature (T_g) are shown in **Figure 4**. For comparison, T_g values relating to the system $20.15[(2.038+x)\text{SiO}_2-(1.457-x)\text{Na}_2\text{O}]-2.6\text{P}_2\text{O}_5-26.95\text{CaO}$ (Kouyate *et al.*, 2013) are also represented in **Figure 4**. A quasi linear increase in glass transition temperature with $\text{Na}_2\text{O}/\text{SiO}_2$ substitution rate is observed in both cases. The T_g is slightly less accentuated in the case of glass enriched in ZnO whatever the silica content.

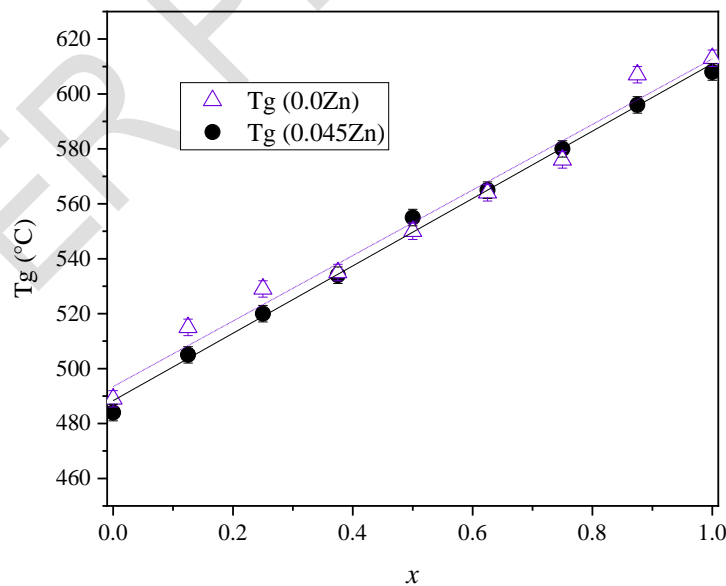


Fig.4.Variations of the glass transition temperature (T_g) in the systems $20.15[(2.038+x)\text{SiO}_2-(1.457-x)\text{Na}_2\text{O}]-2.6\text{P}_2\text{O}_5-26.905\text{CaO}-0.045\text{ZnO}$ and $20.15[(2.038+x)\text{SiO}_2-(1.457-x)\text{Na}_2\text{O}]-2.6\text{P}_2\text{O}_5-26.95\text{CaO}$; $0 \leq x \leq 1$

The glass densities of the system studied and the reference are shown in **Figure 5**. The density of these two systems evolves in the same direction with silica content. Indeed, a decrease in density is observed with silica content. However, the density is slightly lower in the case of Z glass enriched with ZnO, especially at higher silica contents.

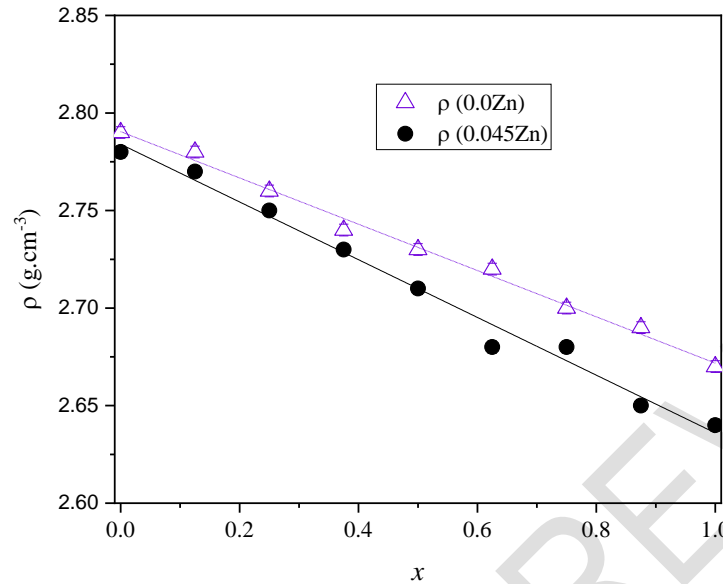


Fig.5. Variation of density with silica content for the systems $20.15[(2.038+x)\text{SiO}_2-(1.457-x)\text{Na}_2\text{O}]-2.6\text{P}_2\text{O}_5-26.905\text{CaO}-0.045\text{ZnO}$ (0.045Zn) and $20.15[(2.038+x)\text{SiO}_2-(1.457-x)\text{Na}_2\text{O}]-2.6\text{P}_2\text{O}_5-26.95\text{CaO}$ (0.0Zn) ; $0 \leq x \leq 1$

3.2 Discussion

The structural state of all glass samples with molar formula $20.15[(2.038+x)\text{SiO}_2-(1.457-x)\text{Na}_2\text{O}]-2.6\text{P}_2\text{O}_5-26.905\text{CaO}-0.045\text{ZnO}$ was characterized by X-ray diffraction. On all diffractograms, flattened diffraction halos (**Figure 2**) were observed, characteristic of diffusion phenomenon in amorphous materials (Nurshen *et al.*, 2022), reflecting the absence of long- distance order. This indicates that the samples produced are devoid of identifiable crystalline species. The samples are indeed amorphous (Hench, 1991). Tg measurements confirm the glassy nature of these samples.

The glass transition is linked to the movement of units in the glass. In this study, each of the thermograms shows a glass transition, confirming the glassy character of these samples (**Figure 3**). The glass transition temperature, Tg, varies from 484°C to 607°C in the bioactive glass system studied at 0.045Zn molar (**Figure 4**). These Tg values are slightly low by about 2 % compared to that at 0.0Zn. These slight variations are due to the association between the increased disruption of the glass lattice caused by a slightly smaller cation Zn (0.074 nm) than Ca (0.099 nm) (Son *et al.*, 2011) and the lower strength of the Zn-O bond.

In doped bioactive glasses and glasses in general, structure correlates with the thermal stability of the glass network (Rajkumar *et al.*, 2010). A very dense structure leads to thermally stable glasses, while a slightly packed structure leads to unstable glasses. In this study, the glass transition temperature increases linearly with the SiO₂ content. Due to its degree of connectivity, silica has the effect of increasing the glass transition temperature (Tg). This increase is in agreement with the results of (Kouyaté *et al.* 2013), which connect the increase in Tg with the increase in the average length of macromolecular chains. Indeed, increasing the average length slows down the freedom of movement of chains relative to each other and promotes network cross-linking. Therefore, Tg increases. However, this cross linking leads to a linear structure that is less compact and therefore less dense.

Furthermore, Tg and density measurements move in the same direction as those of the $20.15[(2.038+x)\text{SiO}_2-(1.457-x)\text{Na}_2\text{O}]-2.6\text{P}_2\text{O}_5-26.95\text{CaO}$ system (Kouyaté *et al.*, 2013). The substitution of CaO by ZnO can influence the structure of the bioactive glasses studied, but both oxides act as modifiers of the glass network, composed of SiO₂ and P₂O₅. They transform bridging oxygens into non-bridging oxygens by breaking bonds. The results showed that the low substitution (0.045 % mol) of CaO by ZnO does not significantly influence the structure of the glass groups studied, also observed by (Lázaro *et al.* 2014) in glasses derived from the SiO₂-CaO-Na₂O-P₂O₅ system.

It has also been suggested that, due to the replacement of CaO by ZnO, changes in the network result from the formation of ZnO_4^{2-} tetrahedral groups requiring Ca ions for charge balancing. This removes cations from the silica network and increases the number of bridging oxygen. The newly formed Si-O-Zn bonds have a significantly lower bond strength than the Si-O-Si bonds in the silicate chain, leading to a decrease in glass transition (Shahrabi. *et al.*, 2011).

These two systems have relatively similar physicochemical characteristics. Density is a property that appears to be closely linked to structural changes in glasses (Montagne *et al.*, 1997). Indeed, glass density is directly related to the density of the elements involved in the system. There is a slight decrease in density (from 2.78 to 2.66 g/cm³) and an increase in average molecular weight with the addition of ZnO in the bioactive glasses studied compared to the reference bioactive glasses (**Figure 4**). This decrease in density of bioactive glasses with 0.045 molar ZnO could be due to the extended structure of the free phosphate glass network resulting from the addition of ZnO. This result is in agreement with that of (Son *et al.*, 2011), which attest that the decrease in density can be attributed to the weak bond strength between Zn-O which, in comparison with bonding between Ca-O which results in higher bond lengths, the expansion network.

4. CONCLUSION

In the present work, thermal analysis methods have been applied to the physicochemical characterization of glasses with a molar formulation of $20.15[(2.038+x)\text{SiO}_2 - (1.457-x)\text{Na}_2\text{O}] - 2.6\text{P}_2\text{O}_5 - 26.905\text{CaO} - 0.045\text{ZnO}$, where $0 \leq x \leq 1$. Materials previously prepared by high temperature melting were analyzed using characterization techniques including X-ray powder diffraction, differential scanning calorimetry and pycnometry. The results highlighted the glassy character of the samples, materialized by the presence of diffusion halos on the X-ray diffractograms of these materials. The results also showed that the glass transition temperature increases slightly with SiO_2 content, while the density decreases slightly. As a result, Zinc additions induce an insignificant change in physicochemical parameters such as Tg and glass density.

REFERENCES

1. Menci PF, Mari A, Charbonneau C, Lefebvre LP, De Nardo L. Aging of Bioactive Glass-Based Foams: Effects on Structure, Properties, and Bioactivity. *Matériaux*. 2019;12:1-13.
2. Jebahi S, Oudadesse H, El Feki H, Rebai T, Keskes H, Pascal P. Antioxidative/oxidative effects of strontium-doped bioactive glass as bone graft, in vivo assays in castrated rats. *Journal of Applied Biomedicine*. 2012;10:195-209.
3. Andersson OH, Karlsson KH, Kangasniemi K, Yli-Urpo A. Models for Physical Properties and Bioactivity of Phosphate Opal Glasses. *Glastechnische Berichte*. 1998;61:300-305.
4. Dickey BT, Kehoe S, Boyd D. Novel adaptations to zinc-silicate glass polyalkenoate cements : The unexpected influences of germanium based glasses on handling characteristics and mechanical properties. *Journal of the Mechanical Behavior of Biomedical Materials*. 2013;8:8-21.
5. Tokudome Y, Otsuka M. Possibility of alveolar bone promoting enhancement by using lipophilic and/or hydrophilic zinc related compounds in zinc-deficient osteoporosis rats. *Biological and Pharmaceutical Bulletin*. 2012;35(9):1496-1501.
6. Diaye M, Degeratu C, Boulter JM, Chappard D. Biomaterial porosity determined by fractal dimensions, succolarity and lacunarity on microcomputed tomographic images. *Materials Science and Engineering: C*. 2013;33(4):2025-30.
7. Feng P, Wei P, Shuai C, Peng S. Characterization of mechanical and biological properties of 3-D scaffolds reinforced with zinc oxide for bone tissue engineering. *PLoS One*. 2014;9(1):87755
8. Chajri S, Bouhazma S, Herradi S, Barkai H, Elabed S, Koraichi SI. (2016). Studies on preparation and characterization of SiO_2 -CaO- P_2O_5 and SiO_2 -CaO- P_2O_5 - Na_2O bioglasses substituted with ZnO. *J Mater Environ Sci*. 2016;188(7):2-97.
9. Ouis M.A. Effect of ZnO on the Bioactivity of Hench's Derived Glasses and Corresponding Glass-Ceramic Derivatives. *Silicon*. 2011;3:177-183.
10. Kouyate A, Ahoussou A.P, Rogez J, Benigni P. Application of Solution Calorimetry to the Prediction of $20.15[(2.038+x)\text{SiO}_2 - (1.457-x)\text{Na}_2\text{O}] - 2.6\text{P}_2\text{O}_5 - 26.95\text{CaO}$ Glass Bioactivity. *Advances in Chemical Engineering and Science*. 2013;3(2):123-129.

11. Mutlu N, Kurtuldu F, Unalan I, Nescakova Z, Kankova H, Galuskova D, Michalek M, Liverani L, Galusek D, Boccaccini AR. Effect of Zn and Ga doping on bioactivity, degradation, and antibacterial properties of borate 1393-B3 bioactive glass. *Ceramics International*. 2022;48:16404–16417
12. Hench LL. Bioceramics: From Concept to Clinic. *Journal of the American Ceramic Society*. 1991;74(7):1487-1510.
13. Son JS, Kim SG, Oh J-S, Appleford M, Oh S, Ong JL, Lee KB. Hydroxyapatite/poly(lactide) biphasic combination scaffold loaded with dexamethasone for bone regeneration. *Journal of Biomedical Materials Research Part A*. 2011;99(4):638–647.
14. Rajkumar G, Aravindan S, Rajendran V. Structural analysis of zirconia-doped calcium phosphate glasses. *Journal of Non-Crystalline Solids*. 2010;356:1432– 1438.
15. Lázaro GS, Santos SC, Xavier Resende C, dos Santos EA. Individual and combined effects of the elements Zn, Mg and Sr on the surface reactivity of a $\text{SiO}_2\cdot\text{CaO}\cdot\text{Na}_2\text{O}\cdot\text{P}_2\text{O}_5$ bioglass system. *Journal of Non-Crystalline Solids*. 2014;386:19–28.
16. Shahrabi S, Hesarak S, Moemeni S, Khorami M. Structural discrepancies and in vitro nanoapatite formation ability of sol-gel derived glasses doped with different bone stimulator ions. *Ceramics international*. 2011;37 : 2737-2746.
17. Montagne L, Palavit G, Delaval R. ^{31}P NMR in $(100-x)(\text{NaPO}_3)_x\text{ZnO}$ glasses. *Journal of Non-Crystalline Solids*. 1997;215:1-10.